

Infrared study of the low-temperature phase transitions in incommensurate Cs_2HgBr_4

A. Jorio

Departamento de Física, Universidade Federal de Minas Gerais, Caixa Postal 702, 30123-970, Belo Horizonte, Minas Gerais, Brazil

P. Echegut

*Centre de Recherches sur la Physique des Hautes Températures—Centre National de la Recherche Scientifique,
1 D avenue de la Recherche Scientifique, 45071 Orléans Cedex 2, France*

N. L. Speziali and M. A. Pimenta

Departamento de Física, Universidade Federal de Minas Gerais, Caixa Postal 702, 30123-970, Belo Horizonte, Minas Gerais, Brazil
(Received 25 November 1998; revised manuscript received 29 December 1998)

In this work we present a complete infrared reflectivity study of the five low-temperature phases of Cs_2HgBr_4 , including the incommensurate structure. Contrarily to the predictions by group theory, no extra modes are observed at the incommensurate (T_I) and lock-in (T_c) phase transitions, showing that the structural changes associated with the modulation does not distort significantly the HgBr_4 tetrahedra. The absence of predicted modes and the presence of a low-frequency relaxation mechanism are discussed in terms of the orientational disorder of the HgBr_4 tetrahedra about the pseudo-hexagonal axis. An important increase of the infrared dielectric constant ϵ'' , observed in the incommensurate phase, is ascribed to the existence of a layered structure of polar domain walls below T_I . [S0163-1829(99)00917-0]

I. INTRODUCTION

Crystals of A_2BX_4 family exhibit a large variety of structural phases, and different physical properties such as ferroelectricity, ferroelasticity, and incommensurability. Cesium mercury bromide (Cs_2HgBr_4) shares some similarities with other compounds from this family, but exhibits particular characteristics that are not yet well understood. The room-temperature structure (phase I) belongs to the $Pnma(D_{2h}^{16})$ space group with $Z=4$.^{1,2} Below $T_I=245$ K, it presents an incommensurate structure (phase II), that is characterized by a wave vector $\mathbf{q}\approx 0.16\mathbf{a}^*$.^{1,2} The wave vector practically does not change in the whole incommensurate interval, contrarily to other well known A_2BX_4 incommensurate compounds. For example, in K_2SeO_4 and Rb_2ZnCl_4 , the modulation wave vector changes with temperature as $\mathbf{q}(T) = n/m[1 + \delta(T)]\mathbf{a}^*$, giving rise to an m fold super structure below the lock-in phase transition. In the case of Cs_2HgBr_4 , modulation wave vector jumps to zero at the lock-in transition ($T_c=232$ K), yielding a commensurate structure (phase III) belonging to the monoclinic $P2_1/n(C_{2h}^5)$ space group with $Z=4$, without the appearance of a superstructure. The crystal undergoes two other phase transitions at about $T_{L1}=165$ K and $T_{L2}=80$ K.^{1,2} Phase IV ($80 < T < 165$ K) belongs to the triclinic $P\bar{1}(C_1^1)$ space group with $Z=4$ and phase V ($T < 80$ K) belongs to the same space group, with $Z=8$.¹

Different experimental techniques have been used to study the sequence of phase transitions of Cs_2HgBr_4 , like nuclear quadrupole resonance (NQR),^{1,3-5} x-ray diffraction,^{2,4,5} NMR,⁶ optical birefringence,^{5,7-10} acoustical studies,¹⁰ specific heat,¹¹ Raman scattering,^{12,13} and dielectric measurements.¹⁴ Besides the appearance of satellite spots in the x-ray-diffraction patterns, the incommensurate phase,

between $245 > T > 232$ K, was also characterized by the broad and typical NMR and NQR bands.³⁻⁶

A recent Raman study of Cs_2HgBr_4 (Ref. 13) showed that the symmetric stretching vibrational mode of the HgBr_4^{-2} tetrahedra (ν_1 mode) exhibits an anomalous behavior, which is in disagreement with group theory predictions. The frequency of the peak associated with the A_g -symmetry ν_1 mode was found to depend on the parallel polarized scattering geometry, and this result was interpreted in terms of the orientational disorder of the HgBr_4^{-2} groups. Besides, the frequency of the A_g -symmetry ν_1 mode propagating along the y crystallographic direction was found to increase continuously in the incommensurate phase, remaining constant below the lock-in phase transition. The observation of a TO-LO splitting in a centrosymmetric structure was ascribed to the presence of a layered structure of polar domain walls.

The above interpretation was confirmed by an x-ray study,² which showed that the room-temperature phase of Cs_2HgBr_4 corresponds to a $Pnma$ disordered structure, where the HgBr_4^{-2} tetrahedra exhibit an orientational disorder about the x direction. The multisoliton regime in the incommensurate phase was evidenced by the coexistence of the lock-in $P2_1/n$ and the incommensurate P_{155}^{Pnma} structures above the lock-in transition. Besides, the lock-in structure was better described by a twinned $P2_1/n$ structure, with the presence of two types of domains.

The purpose of this work is to present an investigation of the Cs_2HgBr_4 by infrared spectroscopy, in the temperature range between 10 and 290 K. Since all the five structures are centrosymmetric, the infrared modes are Raman inactive and therefore the infrared spectra contain complementary information about the lattice dynamics of the Cs_2HgBr_4 crystal at low temperature. The results presented in this work give information about the structural distortions and the role of the

TABLE I. Correlation diagram of the *ungerade* irreducible representations of the point groups in phases I, III, and IV of Cs_2HgBr_4 , and the vibrational modes associated with each representation.

HgBr ₄ vibrational modes	Point groups		
	D _{2h} (Phase I)	C _{2h} (Phase III)	C _i (Phase IV)
$\nu_2, \nu_3, \nu_4, 2\text{lib, ext}$	A _u		
$\nu_1, \nu_2, 2\nu_3, 2\nu_4, \text{lib, 2ext}$	B _{1u} (x)	A _u (x)	A _u (x, y, z)
$\nu_1, \nu_2, 2\nu_3, 2\nu_4, \text{lib, 2ext}$	B _{2u} (z)	B _u (y, z)	
$\nu_2, \nu_3, \nu_4, 2\text{lib, ext}$	B _{3u} (y)		

orientational disorder of the HgBr_4^{2-} anions in the low-temperature phase transitions of Cs_2HgBr_4 .

II. EXPERIMENT

Single colorless crystals of Cs_2HgBr_4 were grown by H. Arend (ETH, Zurich) using the Bridgman method. We have used the convention for the orthorhombic crystal axes in which the lattice parameter a is along the pseudohexagonal x axis and $b < a < c$ [$a = 10.270(2)$ Å, $b = 7.946(1)$ Å, and $c = 13.935(2)$ Å], in accordance to $Pnma$ space group for the structure at room temperature.¹ The samples were cut and polished with faces perpendicular to the crystallographic axes and the orientation of the sample was confirmed by x-ray experiments.

Infrared reflectance spectra were obtained with the light polarized along the three crystallographic axes, in order to observe all modes belonging to all infrared active representations. The spectra have been recorded using an IFS 113 v Bruker interferometer.¹⁵ Measurements were performed between 10 and 450 cm^{-1} , from 10 K up to room temperature.

III. GROUP THEORY ANALYSIS

The present analysis is restricted to the modes related to the HgBr_4^{2-} anions in phases I–V. Since all structural phases of Cs_2HgBr_4 exhibits a centrosymmetric structure, only the modes associated with the *ungerade* irreducible representations are infrared active. Table I shows a correlation diagram of the *ungerade* irreducible representations of the point groups in phases I, III, and IV, and the vibrational modes associated with each representation, according to the factor group analysis presented in Ref. 13. The unit cell in phases I, III, and IV contains four HgBr_4^{2-} tetrahedra and, therefore, 60 degrees of freedom are associated with the vibrations of the HgBr_4^{2-} groups. Twelve of them are related to the translational external modes, 12 to the librational modes, and the remaining 36 are the internal vibrational modes ($4\nu_1, 8\nu_2, 12\nu_3, 12\nu_4$). Phases IV and V have the same point group but the unit cells contain $Z=4$ and $Z=8$ HgBr_4^{2-} units, respectively. Therefore for phase V the number of expected modes is two times the number of modes for phase IV. The basis functions, which give the polarization of the infrared-active modes associated with each representation, are also given in Table I.

At the room-temperature phase I ($Pnma$ or D_{2h}^{16}), the basis functions x , y , and z belong to the different B_{1u} , B_{3u} , and

B_{2u} representations, respectively. Therefore, according to Table I, the x - and z -polarized spectra can exhibit nine distinct modes associated with the HgBr_4^{2-} anions, whereas six modes are expected in the y -polarized spectrum. Figure 1 gives a sketch of the infrared-active internal stretching modes (ν_1 and ν_3) belonging to each representation of Cs_2HgBr_4 at room temperature. These eigenvectors were determined by applying the projectors associated with each representation in arbitrary vectors of the 60-dimensional space.

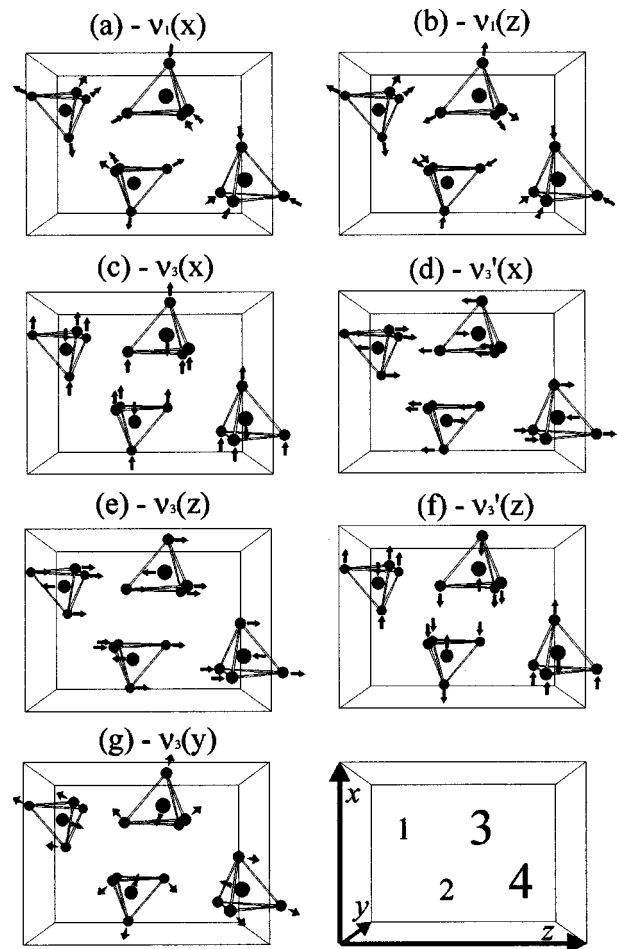


FIG. 1. Schematic picture of the infrared-active stretching internal modes of Cs_2HgBr_4 . The symbols in brackets give the polarization directions x , y , and z , which are associated with the B_{1u} , B_{3u} , and B_{2u} representations, respectively.

Below $T_C=232$ K, the y - and z -polarized modes become associated with the same B_u representation, due to the lowering of the crystal symmetry in phase III (see Table I). Fifteen B_u modes are expected in the y - and z -polarized spectra and $15A_u$ modes are expected in the x -polarized spectrum. For phase IV, all polar modes belong to the same A_u representation, and therefore 30 modes are expected in each one of the three spectra (see Table I). For phase V, due to the doubling of the unit cell, 60 modes are expected in each spectra.

There are different theoretical models which deal with the infrared activity in incommensurate structures and all of them predict the appearance of extra normal modes below the incommensurate phase transition. Generally, these models are based on the multiple folding of the Brillouin zone. According to the superspace-group approach,¹⁶ 15 optic modes of B_{1u} and B_{2u} symmetries and 25 optic modes of B_{3u} symmetry are expected to appear below T_I , considering that the incommensurate phase of Cs_2HgBr_4 belongs to the same P_{1ss}^{Pnma} superspace group as the K_2SeO_4 -type compounds.

IV. RESULTS AND DISCUSSION

A. Room-temperature spectra

The i -polarized infrared reflectance spectra ($i=x, y, \text{ or } z$) were fit using the factorized form of the dielectric function¹⁷

$$\varepsilon_i(\omega) = \varepsilon_{\infty i} \prod_j \frac{\Omega_{i,jLO}^2 - \omega_i^2 + i\omega_i\gamma_{i,jLO}}{\Omega_{i,jTO}^2 - \omega_i^2 + i\omega_i\gamma_{i,jTO}} \quad (1)$$

in which each TO or LO mode j is described by its frequency Ω_j and its damping constant γ_j , and ε_{∞} is the value of the dielectric function in the visible. For normal incidence, the relation between the reflectance $R(\omega)$ and the dielectric function $\varepsilon(\omega)$ is given by

$$R(\omega) = \left| \frac{\sqrt{\varepsilon(\omega)} - 1}{\sqrt{\varepsilon(\omega)} + 1} \right|^2. \quad (2)$$

The oscillator strength $\Delta\varepsilon_{ij}$, which gives the polar character of the mode j can be written as¹⁸

$$\Delta\varepsilon_{i,j} = \varepsilon_{\infty i} \Omega_{i,jTO}^{-2} \frac{\prod_k \Omega_{i,kLO}^2 - \Omega_{i,jLO}^2}{\prod_{k(\neq j)} \Omega_{i,kTO}^2 - \Omega_{i,jTO}^2}. \quad (3)$$

Figure 2 shows the room-temperature infrared reflectance spectra of Cs_2HgBr_4 , polarized along the three crystallographic directions x , y , and z . The solid curves represent the best fit to the experimental data (dots) using Eqs. (1) and (2). Table II shows the parameters (frequencies and damping constants) used to fit the room-temperature spectra. The frequencies of ν_1 and ν_3 stretching internal modes are in the range 150–200 cm^{-1} , whereas the ν_4 bending modes have their frequencies between 60 and 100 cm^{-1} . The ν_2 modes are overlapped with the librational and external modes, below 65 cm^{-1} .

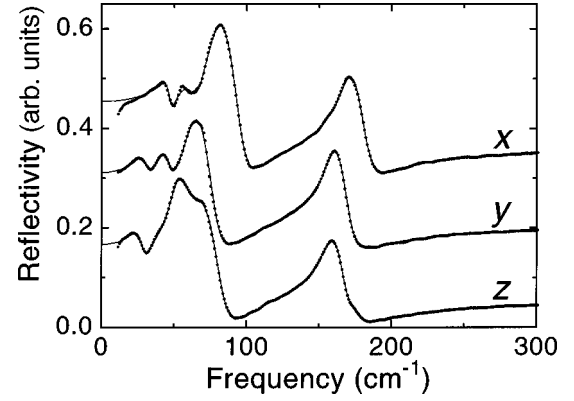


FIG. 2. Room-temperature infrared reflectivity spectra of Cs_2HgBr_4 polarized along the three crystallographic directions. The solid curves represent the best fit to the experimental data (dots).

Note that the number of observed modes is smaller than the number predicted by group theory. According to Table I, two infrared-active ν_1 modes are expected at room temperature, with polarization along x and z directions. However, only one ν_1 mode has been observed, with polarization along the z direction. In the case of a free HgBr_4^{2-} anion, the ν_1 breathing mode is apolar, since the center of the negative charges, associated with the Br atoms, always coincides with the Hg positive charge. However, in Cs_2HgBr_4 , the crystal field might cause a distortion on the tetrahedra, and, in the case of the infrared-active ν_1 modes, the centers of the negative and positive charges do not coincide as the atoms vibrate, giving rise to oscillating dipoles. The oscillator strengths of these modes depend on the distortion of the tetrahedra caused by the crystal field. The fact that only one very weak ν_1 mode is observed in the infrared reflectivity spectra (see Fig. 2 and Table II) suggests that the tetrahedra are not significantly distorted at room temperature.

Let us now discuss the ν_3 modes. According to Table I, only one ν_3 mode is expected in the $B_{3u}(y)$ spectrum, while two ν_3 modes are expected in both the $B_{1u}(x)$ and $B_{2u}(z)$ spectra. However, all the three polarized spectra were fit by introducing only one ν_3 mode in each case. The observation of only one ν_3 mode in the x - and z -polarized spectra can be explained by the analysis of the eigenvectors shown in Fig. 1. Let us consider the two B_{1u} -symmetry $\nu_3(x)$ and $\nu'_3(x)$ modes shown in Fig. 1(c) and 1(d), respectively. The mode shown in Fig. 1(c) [$\nu_3(x)$] exhibits a strong polarization along x direction, since the motions of the atoms are along x . For the mode displayed in Fig. 1(d) [$\nu'_3(x)$] the atoms are vibrating along the z direction, and therefore no net oscillating electric dipole along the x direction would be associated with this mode, if the tetrahedra were not distorted by the crystal field. However, in the case of a distorted tetrahedra, this mode exhibits displacement components also along the x and y directions, and a net oscillating electric dipole appears in the x direction due to the fact that the tetrahedra are localized in a site with m_y symmetry. Therefore the infrared intensity of the $\nu'_3(x)$ mode [Fig. 1(d)] is related to the distortion of the tetrahedra. A similar argument can be used to explain the polar character of the $\nu'_3(z)$ mode displayed in Fig. 1(f).

The experimental observation of only one ν_3 mode in

TABLE II. TO/LO frequencies and damping constants of the room-temperature infrared modes in Cs_2HgBr_4 . The damping constants are between parentheses.

Pol. vector	Frequency (damping constants) of the TO/LO modes (cm^{-1})							
	librational, external, and/or ν_2				ν_4	ν_3	ν_1	
x	-	-	47.9/48.4 (9.0)/(6.5)	-	61.9/63.6 (19.0)/(13.5)	77.6/96.9 (17.0)/(17.0)	169.6/182.6 (16.0)/(16.0)	-
y	31.5/32.4 (12.0)/(10.5)	44.8/47.7 (15.0)/(13.5)	-	-	-	63.0/78.9 (17.0)/(16.0)	158.7/171.4 (15.0)/(15.0)	-
z	29.5/30.5 (13.5)/(10.5)	-	-	54.3/59.7 (14.0)/(16.5)	-	67.3/83.2 (21.0)/(18.0)	158.2/168.7 (16.5)/(14.0)	174.3/176.5 (13.0)/(15.0)

each polarized spectra can be explained by the fact that the tetrahedra are not significantly distorted in the room-temperature phase. Therefore the three ν_3 modes present in the x , y , and z spectra are those in which the vibrations occur along the x , y , and z directions [Figs. 1(c), 1(g), and 1(e)], respectively. The same kind of analysis can be applied to the case of the ν_4 modes in order to understand the appearance of only one ν_4 mode in each polarization, contrarily to the theoretical prediction depicted in Table I.

It is interesting to note that the $\nu_3(y)$ and $\nu_3(z)$ modes have the same TO frequency ($\sim 159 \text{ cm}^{-1}$), whereas the $\nu_3(x)$ mode has the TO frequency up-shifted by 11 cm^{-1} ($\sim 170 \text{ cm}^{-1}$). The same kind of behavior occurs for the ν_4 modes, which also exhibit a strong polar character. The TO frequencies of the ν_4 modes in the y and z spectra are quite similar [$\nu_4(y) \sim 63 \text{ cm}^{-1}$, $\nu_4(z) \sim 67 \text{ cm}^{-1}$] whereas the TO frequency of the x -polarized ν_4 mode is also up-shifted [$\nu_4(x) \sim 78 \text{ cm}^{-1}$]. This result is due to the pseudo-hexagonal character of the room-temperature structure of Cs_2HgBr_4 , since the y - and z -polarized modes would be degenerated in a perfect hexagonal lattice.

The low-frequency modes that appear in all spectra (two in each case) are associated with the vibrations of the Cs^+ ions against the HgBr_4^{2-} groups, the librations of these groups, and the ν_2 internal modes (see Table II). Once again, the pseudo-hexagonal character of the room-temperature structure manifests itself by the similarities in the frequencies of the modes polarized in the y and z directions.

The dielectric constant just below the infrared frequencies can be written as $\epsilon_{0i} = \epsilon_{\infty i} + \sum_j \Delta \epsilon_{ij}$, where the sum is performed for all modes j polarized in the i directions ($i = x, y$, and z). The values obtained for the infrared dielectric constant at room temperature are $\epsilon_{0x} = 5.5$, $\epsilon_{0y} = 5.6$, and $\epsilon_{0z} = 6.0$. Note that these values are smaller than the low-frequency dielectric constants reported by Plesko *et al.*,⁵ that is $\epsilon_{xx} = 6.4$, $\epsilon_{yy} = 12.4$, and $\epsilon_{zz} = 9.6$. The difference is larger for y and z directions and relatively small for the x direction. These differences suggest the existence of a relaxation mechanism, responsible for the increasing on the dielectric constants at low frequencies, and can be related to the presence of an orientational disorder of the tetrahedra groups, reported in Refs. 12 and 13. The relaxation mechanism associated with the rotations of the tetrahedra about the x axis occurs in the basal plane (yz), and therefore induces an increase of the dielectric constants ϵ_{yy} and ϵ_{zz} at low frequencies. Danilov *et al.*¹⁴ reported the temperature dependence of the mean low-frequency dielectric constant using a polycrys-

talline sample of Cs_2HgBr_4 and showed that it decreases below the lock-in phase transition ($T_c = 132 \text{ K}$). This result suggests that the HgBr_4^{2-} orientational disorder decreases in the low-temperature commensurate phases, in agreement with the results obtained by Raman scattering.^{12,13}

As already emphasized, the lack of observation of some predicted modes in the room-temperature spectra is explained by the fact that the tetrahedra are not significantly distorted by the crystal field. This result can be related to the presence of the small-angle orientational disorder of the tetrahedra about the x axis. According to Dmitriev *et al.*,¹² the relaxation time for the tetrahedra reorientation between two equivalent orientations related by the m_y mirror plane is $\tau_R = 5 \times 10^{-13} \text{ s}$ at room temperature. This is a very short time for the dynamics of the tetrahedra between two different orientations in the yz basal plane. Therefore it is reasonable to suppose that the HgBr_4^{2-} tetrahedra are not significantly affected by the static crystal field in each orientation, due to the existence of a fast dynamical orientational disorder. In this sense, the absence of internal modes whose polar character depends on the tetrahedra distortion can be associated with the dynamical orientational disorder of the HgBr_4^{2-} anions.

B. Low-temperature transitions

Figure 3 shows the temperature evolution of the infrared reflectance spectra of Cs_2HgBr_4 between 10 and 280 K. The temperature dependence of the frequencies of the TO internal stretching modes (ν_1 and ν_3) for the three polarizations is shown in Fig. 4. The low-frequency modes ($< 100 \text{ cm}^{-1}$) are not plotted in Fig. 4, since they practically do not exhibit any temperature dependence in the whole temperature interval investigated. Note that only two new modes appear at low temperature, contrary to the group theory analysis (Sec. III) that predicts the appearance of new modes at all phase transitions and in all polarized spectra (see Table I). These two modes appear at the T_{L1} phase transition (phases III-IV) and only in the x -polarized spectrum (see Fig. 3). In the low-frequency range of the spectra (below 100 cm^{-1}) the appearance of new peaks was not observed.

It was already pointed out in the last section that the room-temperature frequencies of the modes vibrating in the basal plane [$\nu_3(y)$ and $\nu_3(z)$] are quite similar due to the pseudo-hexagonal character of the lattice. It is interesting to note that the $\nu_3(y)$ and $\nu_3(z)$ TO frequencies (open circles and full squares in Fig. 4), which are practically the same at

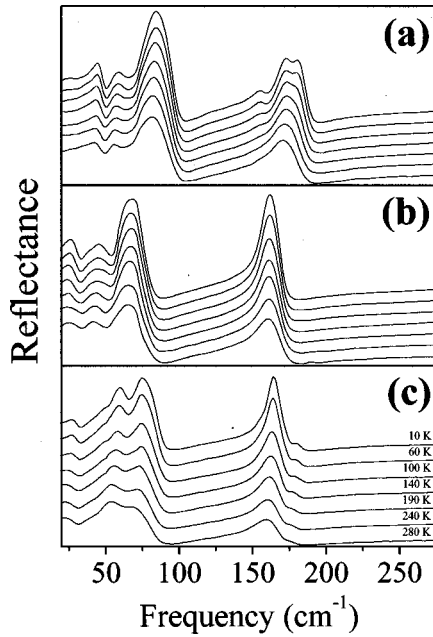


FIG. 3. Temperature evolution of the infrared reflectance spectrum of Cs_2HgBr_4 . (a) x -polarized spectra; (b) y -polarized spectra; (c) z -polarized spectra. (a) and (b) show the spectra at the same temperatures displayed in (c).

room temperature, become different at low temperatures. This behavior reflects the decrease of the pseudo-hexagonal character of the lattice in the low-temperature phases.

According to the theoretical predictions discussed in Sec. III, the appearance of new internal modes is expected below the incommensurate phase transition in A_2BX_4 compounds. In the infrared studies of K_2SeO_4 , Rb_2ZnCl_4 , and K_2ZnCl_4 , new internal modes have been observed below T_I .^{17–19} In the present case, a careful fit of the infrared spectra in the incommensurate phase was performed in order to detect any possible effect of the incommensurability on the spectra line shape. The analysis showed that all spectra could be fit with the same number of oscillators as the room-temperature spectra; no extra modes were observed in the incommensurate phase. Note that the appearance of new internal modes in the incommensurate phase of K_2SeO_4 -type compounds is

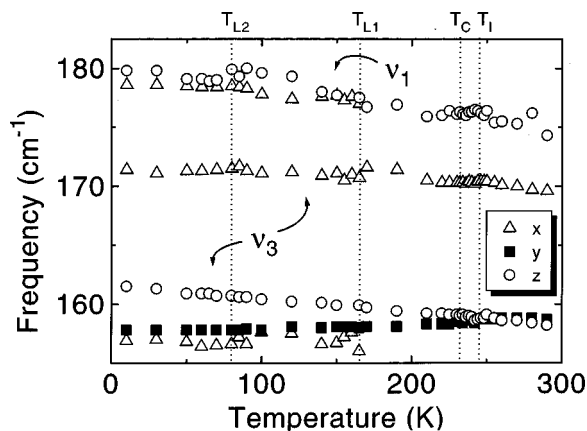


FIG. 4. Temperature dependence of the TO frequencies of the internal stretching modes in the three polarized spectra of Cs_2HgBr_4 .

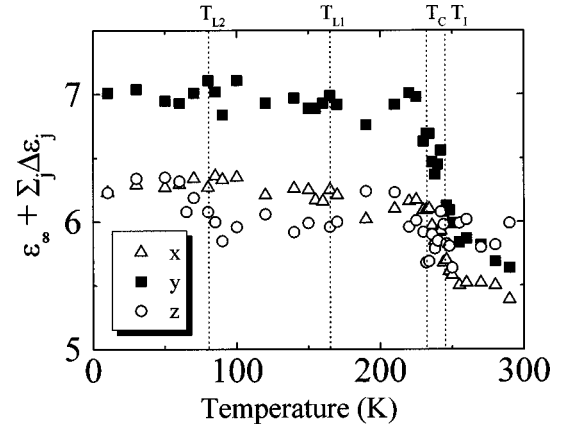


FIG. 5. Temperature dependence of the infrared dielectric constants $\epsilon_{0i} = \epsilon_{\infty i} + \sum_j \Delta \epsilon_{ij}$ along the three crystallographic directions ($i = x, y,$ and z) of Cs_2HgBr_4 .

associated with the triplication of the unit cell, which occurs at the incommensurate-commensurate phase transition.^{17–19} Therefore the absence of extra internal modes in the incommensurate phase of the Cs_2HgBr_4 can be explained by the fact that there is no superstructure below T_c . Moreover, the presence of important disorder effects can obscure the validity of the theoretical predictions concerning the appearance of new modes in the incommensurate phase. This result agrees with the Raman experiments in Cs_2HgBr_4 ,¹³ in which no extra internal modes were observed below T_I .

An interesting question is why new internal modes appear only at the III-IV phase transition. This result can be related to the disorder of the HgBr_4^{2-} tetrahedra at low temperature. As discussed in Sec. IV A, the lack of observation of some predicted modes in the room temperature spectra is attributed to the weak distortion of the tetrahedra, which is associated with the orientational disorder of the HgBr_4^{2-} tetrahedra. According to the Raman study of Cs_2HgBr_4 ,¹³ in the incommensurate and lock-in phases there is a gradual freezing of the orientational disorder, which disappears completely only below the III-IV phase transition ($T_{L1} = 165$ K). In the partially disordered incommensurate and lock-in phases, the changes of the structure does not induce significant distortion of the tetrahedra. On the other hand, the disorder disappear in phase IV, and, in this case, the crystal field deforms the tetrahedra, and gives rise to the appearance of new internal modes in the infrared spectra. These modes correspond to the z -polarized ν_1 and ν_3 modes that become active in x spectra below the phase transition.

Let us now discuss the temperature evolution of the infrared dielectric constant $\epsilon_{0i} = \epsilon_{\infty i} + \sum_j \Delta \epsilon_{ij}$, where $i = x, y,$ or z . Figure 5 shows the temperature dependence of ϵ_{0i} along the three i -crystallographic directions. Note that ϵ_{0x} slightly increases in the incommensurate phase, and this effect is mostly associated with the increase of the high-frequency dielectric constant $\epsilon_{\infty x}$ [see Eq. (3) for $\Delta \epsilon_j$]. On the other hand, ϵ_{0y} exhibits an important increase in the incommensurate phase and remains nearly constant below the lock-in transition. This effect is mainly due to the increase of the oscillator strength of the two lowest-frequency modes in y -polarized spectra.

The important increase of the oscillator strength for the y -polarized modes is ascribed to the appearance of an extra mechanism of polarization along y direction, which increases the effective charges of the y -polar modes and, consequently, their TO-LO splitting. A possible explanation for this result is the presence of a layered structure of polar domain walls which appears below T_I . The Cs_2HgBr_4 crystals present an easy cleavage plane perpendicular to the z axis, since the bonding between atoms in that direction is weaker than in other directions. According to the symmetry analysis presented in Ref. 13, the domain wall parallel to this cleavage plane exhibits a macroscopic polarization along the y direction. This macroscopic polarization might be responsible for the increase of the TO-LO splitting observed for the y -polarized infrared modes, and thus for the jump of ϵ_{0y} below the incommensurate phase transition.

V. CONCLUSION

In this work we present a complete infrared reflectivity study of the five low-temperature phases of Cs_2HgBr_4 , between 10 and 290 K. The number of observed modes in the infrared reflectivity spectra is always smaller than the number predicted by group theory, and no extra modes were observed in the incommensurate (II) and lock-in (III) phases. This result can be related to the order-disorder character of the phase transitions, in which the changes in the crystal structure are mostly due to the gradual freezing in the orientational dynamics of the tetrahedra. In the disordered or par-

tially disordered phases I, II, and III, the tetrahedra are not significantly distorted by the crystal fields, and therefore a number of predicted modes are not observed. The appearance of two modes occurs only in III-IV phase transition, and is associated with the freezing of the orientational disorder below T_{L1} .

The difference between the infrared and the low-frequency dielectric constants in the yz basal plane is ascribed to the existence of a relaxation mechanism associated with the orientational disorder of the HgBr_4^{2-} groups about the pseudo-hexagonal x axis. This difference decreases at low temperature, in agreement with the reported gradual freezing of the orientational disorder below the incommensurate transition.¹³ The infrared dielectric constant along the y direction ϵ_{0y} exhibits an important increase at the incommensurate phase and remains constant below the lock-in transition. This result is interpreted as a consequence of the presence of a layered structure with polar domain walls which appears below T_I .

ACKNOWLEDGMENTS

The authors would like to acknowledge Professor P. Saint-Gregoire, Dr. Igor Luk'Yanchuk, C. B. Pinheiro, Dr. P. Simon, and D. S. Meneses for helpful discussions, and J. V. Fonseca and A. Blin for technical assistance. This work was supported by the Brazilian Agencies CAPES, FAPEMIG, CNPq and FINEP, and by CNRS (France).

-
- ¹D. Altermatt, H. Arend, V. Gramlich, A. Niggli, and W. Petter, *Acta Crystallogr., Sect. B: Struct. Sci.* **40**, 347 (1984).
- ²C. B. Pinheiro, A. Jório, M. A. Pimenta, and N. L. Speziali, *Acta Crystallogr., Sect. B: Struct. Sci.* **54**, 197 (1998).
- ³A. V. Bondar, S. M. Ryabchenko, and A. Yu. Khalakhan, *Sov. Phys. Solid State* **30**, 1315 (1988).
- ⁴S. Plesko, R. Kind, and H. Arend, *Phys. Status Solidi A* **61**, 87 (1980).
- ⁵S. Plesko, V. Dvorak, R. Kind, and A. Treindl, *Ferroelectrics* **36**, 331 (1981).
- ⁶A. A. Boguslavskii, Yu. N. Ivanov, A. I. Krieger, A. K. Moskalev, V. I. Pakhomov, and R. Sh. Lotfullin, *Phys. Status Solidi B* **161**, K49 (1990).
- ⁷A. V. Kityk, O. M. Mokry, V. P. Soprunyuk, and O. G. Vlokh, *J. Phys.: Condens. Matter* **5**, 5189 (1993).
- ⁸O. G. Vlokh, V. S. Zhmurko, I. I. Polovinko, and S. A. Sveleba, *Sov. Phys. Solid State* **33**, 1758 (1991).
- ⁹O. G. Vlokh, A. V. Kityk, O. M. Mokryi, V. V. Kirilenko, I. D. Olekseyuk, and S. A. Piroga, *Sov. Phys. Solid State* **31**, 901 (1989).
- ¹⁰O. G. Vlokh, V. G. Gribik, A. V. Kityk, O. M. Mokryi, I. D. Olekseyuk, and S. A. Piroga, *Sov. Phys. Crystallogr.* **35**, 873 (1990).
- ¹¹V. V. Petrov, A. Yu. Khalakhan, V. G. Pitsyuga, and V. E. Yachmenev, *Sov. Phys. Solid State* **30**, 906 (1988).
- ¹²V. P. Dmitriev, Yu. I. Yuzyuk, Yu. I. Durnev, L. M. Rabkin, E. S. Larin, and V. I. Pakhomov, *Sov. Phys. Solid State* **31**, 770 (1989).
- ¹³A. Jório, M. S. S. Dantas, C. B. Pinheiro, N. L. Speziali, and M. A. Pimenta, *Phys. Rev. B* **57**, 203 (1998).
- ¹⁴V. V. Danilov, V. V. Onopko, A. V. Boydanova, and G. Shul'ga, *Sov. Phys. Solid State* **33**, 1459 (1981).
- ¹⁵F. Gervais, in *Infrared and Millimeter Waves*, edited by K. J. Button (Academic, New York, 1993), Vol. 8, p. 288.
- ¹⁶Th. Rasing, P. Wyder, A. Janner, and T. Janssen, *Phys. Rev. B* **25**, 7504 (1982).
- ¹⁷F. Gervais and P. Echegut, in *Incommensurate Phases in Dielectrics*, edited by R. Blinc and A. P. Levanyuk (North Holland, Amsterdam, 1986), p. 337.
- ¹⁸P. Echegut, F. Gervais, and N. E. Massa, *Phys. Rev. B* **31**, 581 (1985).
- ¹⁹P. Echégut, F. Gervais, and N. E. Massa, *Phys. Rev. B* **30**, 6039 (1984).